http://www.press.ierek.com

ISSN (Print: 2357-0849, online: 2357-0857)

Environmental Science and Sustainable Development

Research Paper
Received:13 October 2025, Accepted: 25 November 2025, Published online: 31 December 2025
DOI: 10.21625/essd.v10i4.1253

Impact of Garden Greening on the Outdoor Thermal Environment of Buildings - a Case Study of Japanese Residential Houses

Fulin Jia[1], Bart Julien Dewancker[2], Weijun Gao[3]

[1] *Doctor student, Department of Architecture, The University of Kitakyushu, Japan*

[2] *Professor, Department of Architecture, The University of Kitakyushu, Japan*

[3] *Professor, Department of Architecture, The University of Kitakyushu, Japan*

Abstract

Garden greening not only enhances the aesthetic value of residential buildings but also plays a critical role in improving microclimates and regulating the outdoor thermal environment. In Japan, incorporating garden greenery has become a prevalent feature of residential architecture. However, limited empirical research exists that systematically compares how different types of vegetation influence outdoor thermal conditions in Japanese residential gardens. This study addresses that gap by examining the impact of varying greening configurations on air temperature and relative humidity. Field measurements were conducted during both summer and winter in two traditional residential gardens located in Kitakyushu, southern Japan, using four monitoring points representing different greening structures. Results revealed that air temperature and relative humidity showed consistent patterns across seasons, with Measurement Point A (combining herbaceous plants, shrubs, and trees) yielding the lowest average temperature and highest humidity, while Point D (no greening) exhibited the highest temperature and lowest humidity. The findings confirm that vegetation type significantly affects the microclimate. Notably, while vegetation improves outdoor comfort in summer by reducing heat stress, it may worsen thermal comfort in winter by retaining humidity and lowering temperature. This study provides evidence-based insights into the dual seasonal effects of garden greening, offering valuable guidance for sustainable residential garden design in Japan's urban context.

Keywords

Garden greening, Outdoor thermal environment, Types of greening, Japanese residential houses;

1. Introduction

Urbanization has dramatically reshaped the landscape of human settlements worldwide, altering both the built environment and the natural systems that sustain it. One of the most pressing consequences of urban expansion is the modification of local and regional climates, manifested most prominently in the urban heat island (UHI) phenomenon. This effect arises from the replacement of natural land surfaces with impervious materials such as asphalt and concrete, which absorb and retain heat while reducing evaporative cooling. As global warming continues to amplify thermal stress in cities, there is a growing need for effective strategies to mitigate rising temperatures and improve outdoor comfort (Bowler et al., 2010). Within this context, vegetation has been widely recognized as a key element in regulating microclimates and enhancing thermal environments. Urban greening, including trees, shrubs, and

herbaceous vegetation, provides multiple ecosystem services that extend beyond aesthetics to climate adaptation and human health.

A substantial body of research has demonstrated that vegetation contributes to microclimate regulation by lowering air temperature, increasing relative humidity, and modifying wind flow. For instance, Shashua-Bar et al. (Shashua-Bar et al., 2011) found that trees and grass significantly improved outdoor thermal comfort in hot-arid environments, highlighting the importance of vegetation type and structure. Similarly, Ng et al. (Ng et al., 2012) observed that greening in high-density Hong Kong reduced ambient air temperature by several degrees, illustrating the cooling potential of vegetation in compact urban areas. Hamada and Ohta (Hamada & Ohta, 2010) further emphasized the seasonal variability of greening effects, showing that urban green areas provided cooling benefits in summer while influencing thermal conditions differently during winter. These findings collectively underscore that vegetation moderates the urban thermal environment through processes such as shading, evapotranspiration, and wind modification, yet the magnitude of these effects depends on plant type, spatial configuration, and seasonal dynamics.

Despite global advances in understanding vegetation's role in thermal regulation, the specific context of residential gardens remains underexplored (Lin & Li, 2025). Residential gardens are unique micro-landscapes that integrate vegetation within the immediate living environment, offering not only ecological benefits but also cultural and social value (Shen L et al. 2022). In Japan, residential gardens are particularly significant, given the country's long-standing tradition of integrating nature into the domestic sphere. Japanese gardens are characterized by their careful design, use of diverse plant species, and symbolic representations of natural landscapes (Heikkilä & Hautamäki, 2024). Beyond their aesthetic and cultural importance, they are increasingly recognized as potential moderators of microclimate at the household scale. Nevertheless, most of these studies have been conducted at the neighborhood or city scale, leaving a gap in the literature regarding small-scale residential gardens.

A related issue concerns the diversity of vegetation types within gardens and their differential contributions to thermal environments. Morakinyo et al. (Morakinyo et al., 2016) demonstrated, through simulations, that tree configurations and planting patterns in street canyons had significant effects on microclimate and human thermal comfort. These insights are directly relevant to residential gardens, where design choices regarding plant type—trees, shrubs, or herbaceous vegetation—may influence temperature and humidity in distinct ways. However, the vast majority of studies focus on broader urban green spaces such as parks (Spronken-Smith & Oke, 1999) or street greenery (Klemm et al., 2015), while systematic comparisons among different garden vegetation types remain rare. Furthermore, the thermal environment of Japanese gardens has seasonal particularities, as the cooling and humidifying effects of vegetation in summer may conversely exacerbate cold stress in winter, yet this dual effect has seldom been empirically documented.

These gaps highlight the need for focused investigations into the microclimatic functions of residential garden greening in Japan. Unlike public parks or urban forests, residential gardens are private and highly localized, yet they collectively represent a substantial proportion of urban greenery in Japanese cities. Their potential contributions to outdoor thermal comfort are therefore not trivial, particularly as climate change increases the frequency of heat waves. Moreover, the scarcity of empirical measurements comparing multiple vegetation types under different seasonal conditions poses a limitation for both scholars and practitioners seeking evidence-based guidelines for garden design. By addressing these gaps, research on residential garden greening can advance understanding of how small-scale vegetation systems influence microclimate, while also informing sustainable landscape practices in urban environments.

The present study aims to contribute to this emerging field by examining the effects of different types of garden greening on the outdoor thermal environment in a traditional Japanese residential garden. Through systematic field measurements conducted in both summer and winter, this research evaluates variations in air temperature and relative humidity across multiple garden settings characterized by distinct vegetation types. By comparing sites with herbaceous plants, shrubs, trees, and non-greened areas, the study identifies the relative performance of different greenery configurations in moderating microclimatic conditions. In doing so, it provides novel empirical evidence of the seasonal dual role of greenery—beneficial for cooling and humidifying in summer but potentially detrimental to thermal comfort in winter. This nuanced understanding enriches the global discourse on urban greening by

emphasizing the importance of scale, vegetation type, and seasonal dynamics, while also responding to the specific cultural and environmental context of Japanese residential gardens. Ultimately, the findings contribute both to academic knowledge and to practical strategies for enhancing thermal comfort and sustainability in residential landscapes.

To address the identified gaps, this study seeks to answer the following research questions:

(1) How do different types of garden greening—ranging from multi-layered vegetation to no greening—affect the outdoor thermal environment in Japanese residential gardens across seasons?

(2) Does the structural complexity of vegetation lead to more stable and comfortable microclimatic conditions, particularly in terms of air temperature and relative humidity?

Based on previous literature and field observations, the study hypothesizes that multi-layered vegetation (combining herbaceous plants, shrubs, and trees) provides stronger thermal regulation and humidity stability, especially in summer, while in winter, such vegetation may lead to lower perceived comfort due to moisture retention and cooling effects. These hypotheses guide empirical analysis and frame the study's contribution to urban microclimate research and sustainable residential landscape design.

2. Methodology.

2.1 Field measurement location.

The experimental sites for this study were located at two residences, A and B with gardens in Yahatanishi-ku, Kitakyushu, Fukuoka Prefecture, southern Japan (Figure 1), in which the garden of Residence A was a green garden with plants, and the garden of Residence B was not green (Figure 2). The straight-line distance between Residence A (33° 53′ N,130° 42′ E) and Residence B (33° 52′ N,130° 42′ E) is 1.77km, where Residence A is set up as the experimental group and Residence B is set up as the control group. The climate of the area where the two courtyards are located belongs to the temperate marine monsoon climate. The average annual temperature is 16.6°C, the rainfall is abundant throughout the year, with an average precipitation of 1720.5 mm, the yearly average wind speed is 2.1 m/s, the total annual sunshine duration is 1835.7 h, the summer temperature is high, and the humidity is high, and the winter is warm (Zhang et al., 2021).

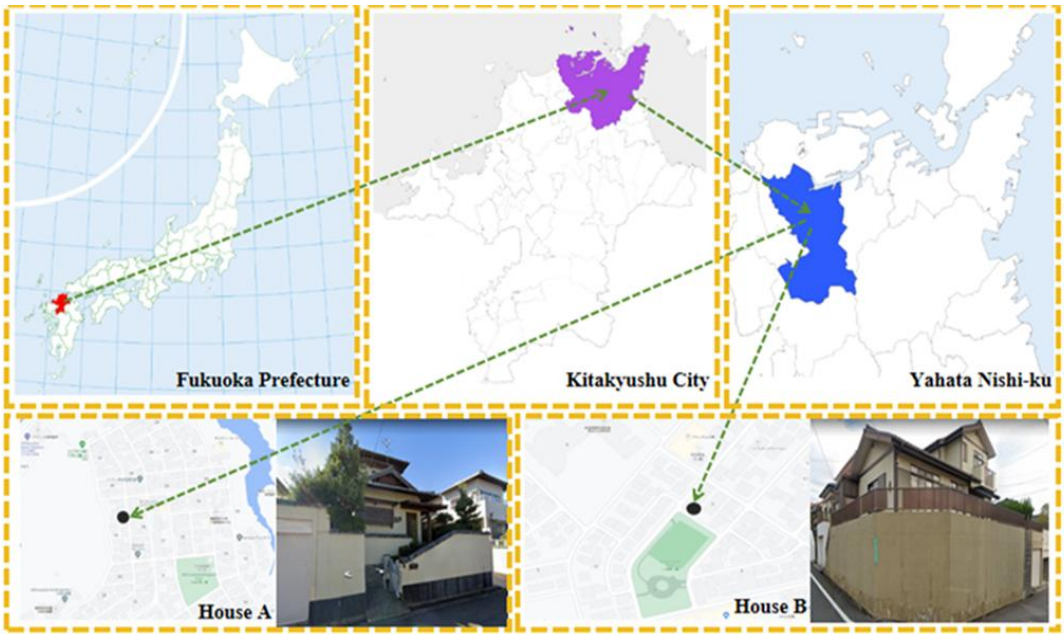

Figure 1 Experimental sites (source: by authors).

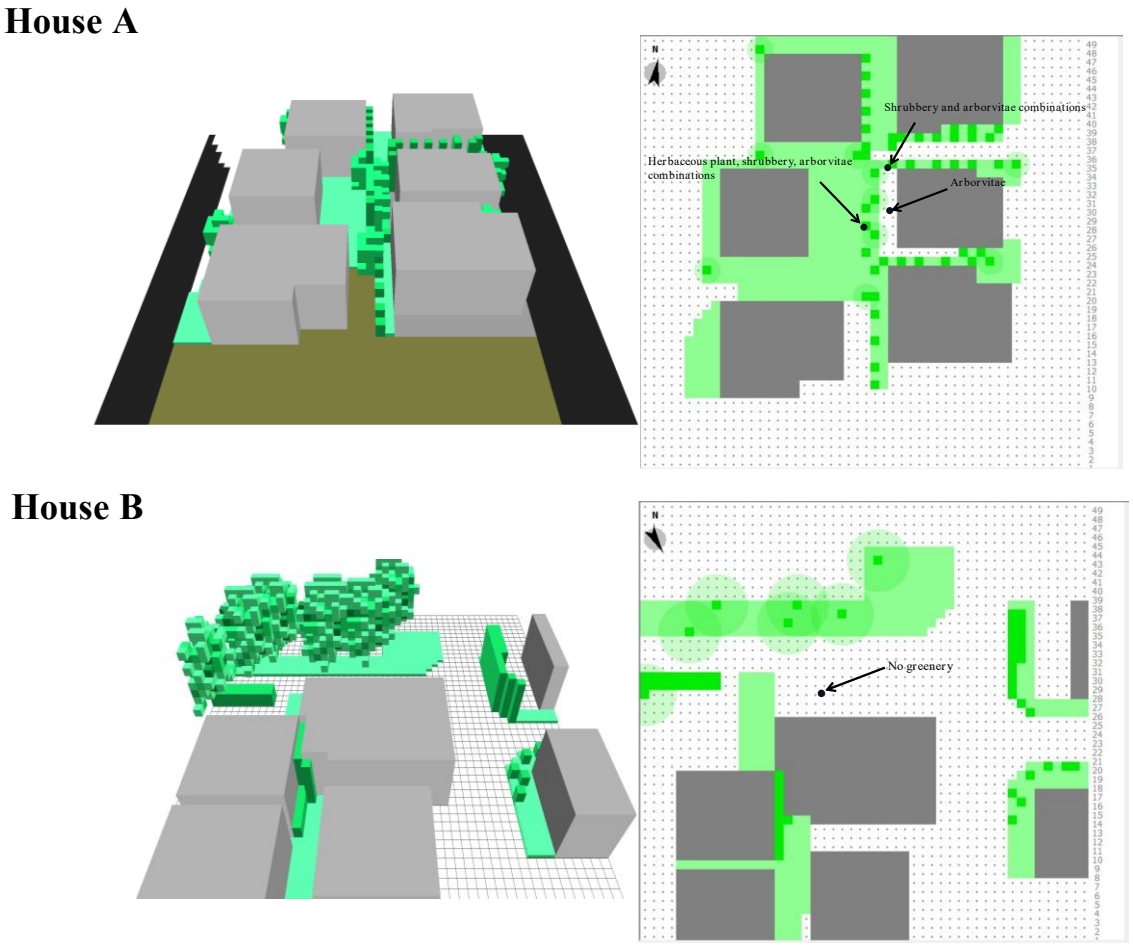

Figure 2 Schematic diagram of the 3D modeling of the experimental site (source: by authors).

2.2 Field measurement procedure

The experiment involved data collection at different measurement points within two traditional Japanese residences (detailed measurement points are listed in Table 1). These residences are geographically close, share similar courtyard structures and building orientations, and are both located at comparable distances from the local meteorological station. Therefore, these two residences were selected as subjects for the comparative experiment. Winter measurements were conducted from January 26 to February 9, 2023, while summer measurements spanned July 19 to August 8, 2023. These periods corresponded to the lowest and highest average temperatures during winter and summer, respectively, at the experimental sites. Experimental measurement instruments were deployed at four distinct monitoring points (Table 1), each positioned 1.1 meters above ground level (equivalent to the center of gravity height of an adult standing upright) (Cannistraro & Trancossi, 2019). Measurements were conducted using the TR-72wb temperature and humidity recorder (instrument specifications in Table 2), configured to measure and log air temperature (AT) and relative humidity (RH) every half hour.

These two residences were chosen not only for their proximity but also because they possess similar garden orientations, surrounding building heights, and minimal artificial shading, which reduces potential confounding factors in microclimatic measurements. Both gardens are oriented towards the southeast and are not shaded by adjacent structures, ensuring consistent exposure to solar radiation. This comparability enhances the reliability of the site-based comparison.

In terms of data analysis, after the collection phase, all air temperature and relative humidity records were averaged for each hour to reduce noise caused by short-term fluctuations. Subsequently, daily mean, maximum, and minimum values were extracted and used for cross-site comparisons. Descriptive statistics were computed for each measurement point, and diurnal patterns were visualized using time-series plots. Additionally, intra-site and inter-site variability was evaluated to identify differences between greening types and assess the seasonal impact on thermal

performance. While this study emphasizes empirical observation, basic statistical tools were used to support pattern recognition and interpretation.

Table 1: Description of greening types at each measurement point (source: by authors).

Point name	Type of greening
A	Herbaceous plants, Shrubs, Trees
B	Shrubs, Trees
C	Trees
D	No greening

Table 2: Basic information on measuring instruments (source: by authors).

Name of instrument	Measurement parameters	Measurement range	Measurement accuracy
TR-72wb	Air temperature Ta	0-55°C	±0.5°C
	Relative humidity RH	10-95%RH	±5%RH (at 25° C,50%RH）

3. Results and discussion

3.1 Measurement of outdoor thermal environments at different measurement points during winter

Figure 3 presents the continuous 24-hour air-temperature variations measured at the four monitoring points on the coldest day of observation. The data clearly show the diurnal evolution of temperature under different greening configurations. From midnight until approximately 08:30, all four trajectories display a gradual increase, a typical signature of the nocturnal inversion layer dissipating with the approach of sunrise. During this period, the relative differences between the four sites remain modest, although minor deviations are already observable.

At 08:00, persistent snowfall begins to influence the microclimate. Sensor D, located at the site without any greening, responds most rapidly, showing an immediate 0.8 °C decline. In contrast, the three vegetated sites—A (herbaceous plants, shrubs, and trees), B (shrubs and trees), and C (trees only)—continue their slow upward trend until about 08:30 before the cooling effect becomes evident. This difference suggests that the presence of vegetation moderates the immediate response to snowfall, producing a short delay in the cooling pattern.

Once snowfall ceases at 11:00, all four trajectories show a sharp rebound. Each site recovers most of the earlier temperature loss within a relatively short timeframe. The recovery is broadly synchronized, although small differences remain among the sensors. Between 12:00 and 12:30, a brief shower produces a coordinated decline across all four measurement points, with a drop of approximately 1.4 °C recorded. After this episode, temperatures resume their ascent as insulation effects dominate, leading to the daily maximum by around 15:30. At this point, the inter-sensor range is approximately 3.2 °C, reflecting clear differentiation between greening types.

From 15:30 onwards, radiative cooling becomes the prevailing process. The four curves begin a steady decline, continuing until midnight. Throughout this phase, vegetation composition exerts an observable influence on relative rankings. Sensor A, which combines herbaceous plants, shrubs, and trees, becomes the coldest point from 06:30 onward and maintains this position until the end of the record. Sensors B and C follow similar paths, remaining slightly warmer than A but cooler than D.

Sensor D, the non-vegetated site, exhibits the greatest volatility across the day. It records the lowest temperatures between 00:00 and 02:00, then shifts upward to rank above C between 02:00 and 07:00. From 07:00 to 16:30, D becomes the warmest of all four sensors, diverging notably from the vegetated points during the period of solar input and post-snowfall recovery. After 16:30, its trajectory falls below C, and for the remainder of the evening, it oscillates around B, generally positioned slightly beneath it. This pattern underlines the stronger variability observed in the non-green condition compared with the more consistent behaviors of the vegetated sites.

Quantitative analysis of the recorded data further supports these qualitative observations. On the coldest day, the average air temperature at Point A (with herbaceous plants, shrubs, and trees) was 0.9 °C lower than that of Point D (no greening), with a mean of 0.8 °C at Point A versus 1.7 °C at Point D. The daily temperature range at Point D reached over 8.2 °C, nearly twice the amplitude observed at Point A (4.6 °C), indicating a much higher diurnal fluctuation in the absence of vegetation. In contrast, Points B and C showed intermediate values, with average temperatures of 1.2 °C and 1.7 °C, respectively. These quantitative differences confirm that increased vegetation complexity correlates with lower average temperatures and more stable thermal profiles, reinforcing the interpretation that greening mitigates both temperature extremes and rapid fluctuations under cold conditions.

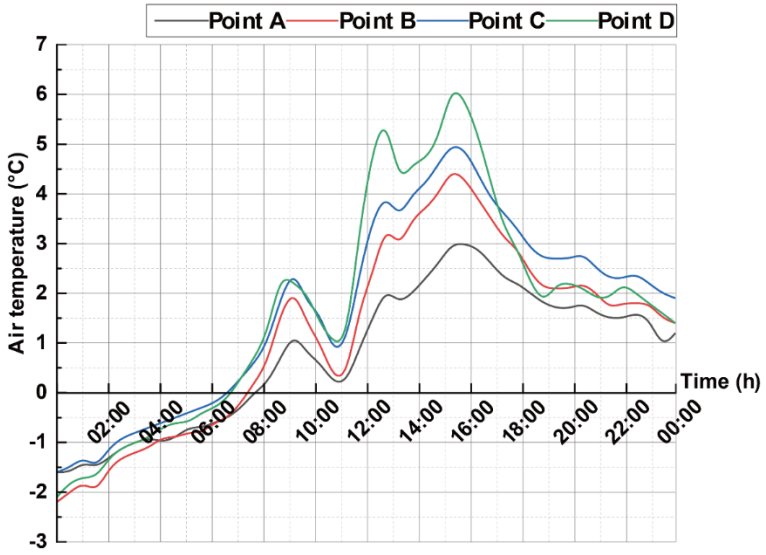

Figure 3 Air temperature measurement diagram for January 26, 2023 (source: by authors).

Figure 4 depicts the 24-hour relative humidity (RH) trajectories observed at the four monitoring points, highlighting the dynamic interplay between vegetation cover and atmospheric processes. From 00:00 to 01:30, all four traces remain nearly horizontal, fluctuating minimally around 82 %. This stability reflects a nocturnal equilibrium phase. Between 01:30 and 03:00, however, a brief evaporation episode drives RH downward, with values reaching the nightly minimum of approximately 75 %. Subsequently, moist advection reverses the trend, lifting RH steadily from 04:00 to 05:30 until values exceed 88 %. During this recovery, the four sensors exhibit synchronized movement, and conditions stabilize at high humidity until 07:30.

The onset of snowfall at 08:30 triggers a sharp divergence in responses. Sensors A and B, associated with herbaceous plants, shrubs, and trees (A) or shrubs and trees (B), respond first, registering a rapid surge to 95 % within 20 minutes. Sensors C (trees only) and D (no greening) follow more gradually, indicating a slightly delayed moisture uptake. By 11:00, sensors B, C, and D approach saturation levels near 100 %, while sensor A, though also reaching near-saturation, peaks one hour later at 12:00. The delay at A may be linked to the combined vegetation layers influencing micro-scale humidity retention.

From 12:00 to 15:30, a pronounced drying phase dominates. During this interval, RH declines significantly across all sensors, reaching values between 35 % and 60 %, depending on location. This marks the daily minimum for each monitoring point. The drop is most evident at sensor D, which registers one of the lowest RH values in the group, consistent with the absence of greening at that site. Sensors A, B, and C retain relatively higher levels, though all experience substantial reductions.

After 15:30, a secondary moisture pulse occurs. RH begins to climb again, peaking near 19:00, with notable increases across all sensors. Thereafter, values decline gradually until 22:00. From 22:00 onwards, slight radiative cooling promotes another modest rise in RH, bringing the day's cycle to a close with readings around 70 %.

Throughout the 24 hours, the sensors demonstrate consistent differences associated with vegetation type. Sensor A, representing the site with the most diverse greening (herbaceous, shrubs, and trees), maintains the highest RH values and exhibits the least variability. Sensor D, located in the non-greened area, shows the greatest volatility, tracking below A and B from 00:00 to 04:00, becoming the lowest of the four from 04:00 to 17:00, and then oscillating markedly thereafter. Sensors B and C follow parallel trajectories, with C consistently registering 3–8 % lower RH than B across all corresponding times. These consistent patterns indicate distinct microclimatic behaviors among the four measurement points, with vegetation composition playing a central role in shaping RH variability.

Quantitative analysis of relative humidity over the 24 hours further illustrates these patterns. Sensor A consistently recorded the highest average RH at 80.3%, while Sensor D exhibited the lowest at 70.9%, indicating a substantial difference of 9.4 percentage points attributable to vegetation presence. During the afternoon drying phase (12:00–15:30), the minimum RH at Point D dropped to 59.4%, compared to 78.7% at Point A, reflecting a greater moisture retention capacity in vegetated areas. Additionally, the standard deviation of RH across the day was lowest at A (±8.09%) and highest at D (±10.36%), confirming that diverse vegetation not only elevates humidity levels but also buffers diurnal fluctuations. These numerical differences support the interpretation that vegetation—especially multi-layered plant structures—plays a decisive role in enhancing humidity stability and mitigating abrupt environmental shifts.

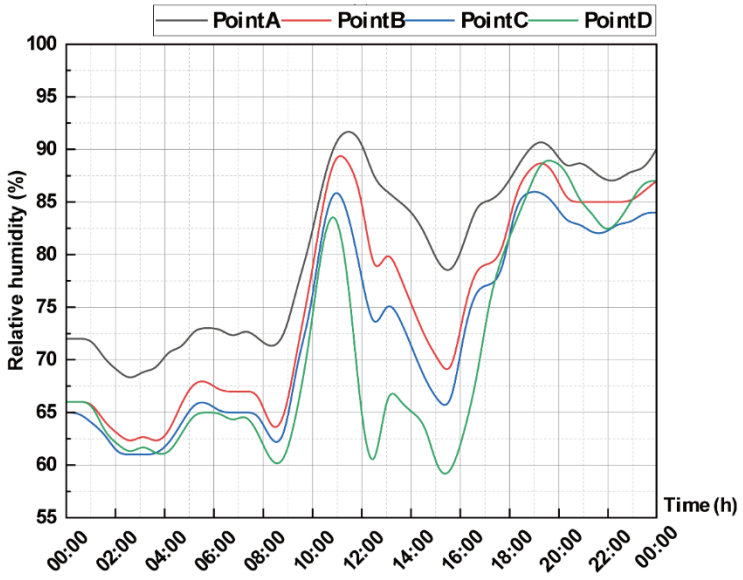

Figure 4 Air temperature measurement diagram for January 26, 2023 (source: by authors).

3.2 Measurement of outdoor thermal environments at different measurement points during summer

Figure 5 illustrates the complete 24-hour air-temperature evolution measured by the four sensors on 28 July 2023, a representative hot summer day. From midnight until 05:00, all sensors undergo a uniform cooling phase dominated by radiative heat loss to the night sky. Temperatures decline steadily to approximately 26 °C, with no significant divergence among sites. This initial cooling sets the stage for the subsequent daytime warming phase, during which differences in surface cover and vegetation composition lead to pronounced variability.

After 05:00, all sensors begin to register rising temperatures, but the rates and amplitudes vary considerably. Sensor D, located in the non-greened area on dark asphalt, responds most rapidly to incoming solar radiation. Its temperature increases almost linearly throughout the morning, culminating in an extreme maximum of 50.1 °C at 15:00. This peak is the highest among the four monitoring points and highlights the absence of any moderating influence from vegetation. Following this maximum, sensor D enters a steady decline that continues into the nighttime hours.

Sensors A and B, both situated in vegetated zones, display more moderate responses. Sensor A, which integrates herbaceous plants, shrubs, and trees, records a peak of 35.2 °C at 08:30. Sensor B, covered by shrubs and trees, follows a similar trajectory but reaches a higher maximum of 37.8 °C at the same time. After reaching these morning peaks, both sensors begin a gradual decline, maintaining smoother and more stable curves compared to the more volatile behavior of sensor D. The early peaks observed at A and B suggest that dense vegetation can regulate surface and near-surface temperatures by limiting excessive heat accumulation.

Sensor C, representing the site with tree-only coverage, shows a more complex trajectory. Between 07:00 and 07:30, a sudden temperature drop occurs, followed by a rebound at 08:00 and another decrease until 09:00. Thereafter, temperatures climb more gradually, reaching a maximum of 38.6 °C at 13:30, before declining alongside the other sensors in the evening. The fluctuations observed at sensor C likely reflect localized meteorological factors, such as intermittent shading and cloud cover, which interrupt the otherwise steady warming trend.

Across the diurnal cycle, the amplitude of change differs substantially among the four sensors. Sensor D exhibits the largest thermal amplitude and the steepest gradients, underscoring the absence of vegetation as a key factor in heat accumulation and release. Sensor C ranks second in variability, while sensors A and B show the smallest amplitudes and the most synchronous patterns. At 15:00, the temperature contrast between D (50.1 °C) and A (33 °C) reaches 16.9 °C, clearly demonstrating the extent of intra-site variability within the same garden environment. These results indicate that the presence and type of vegetation substantially influence temperature dynamics across space and time, even under identical meteorological conditions.

Quantitative analysis confirms the observed thermal divergence. Over the 24 hours, Sensor D recorded the highest average air temperature at 33.6 °C, while Sensor A recorded the lowest at 28.5 °C, indicating a mean difference of 5.1 °C. The daily maximum reached 50.1 °C at D versus 35.2 °C at A, and the thermal amplitude (difference between daily max and min) was 24.1 °C at D but only 11.7 °C at A, revealing the strong buffering effect of dense vegetation.

Statistically, the standard deviation of hourly temperature at D was 7.4°C, nearly double that of A (3.8 °C), suggesting greater thermal volatility in the non-vegetated zone. Daytime (06:00–18:00) averages further emphasize the disparity: D averaged 38.6 °C, A only 31.5 °C, a striking 7.1°C gap. Nighttime temperatures (00:00–05:00 and 19:00–24:00) showed reduced variation, with all points converging around 26–28 °C.

The substantial cooling in vegetated areas is primarily attributed to canopy shading, evapotranspiration, and reduced ground heat absorption. Sensor A's three-layer vegetation structure maximizes shading while enhancing latent heat loss through transpiration, which mitigates daytime heating. In contrast, D's bare asphalt surface absorbs and re-emits heat with minimal delay. These differences demonstrate how vegetation type and structure exert microclimatic control even under identical macro-environmental conditions.

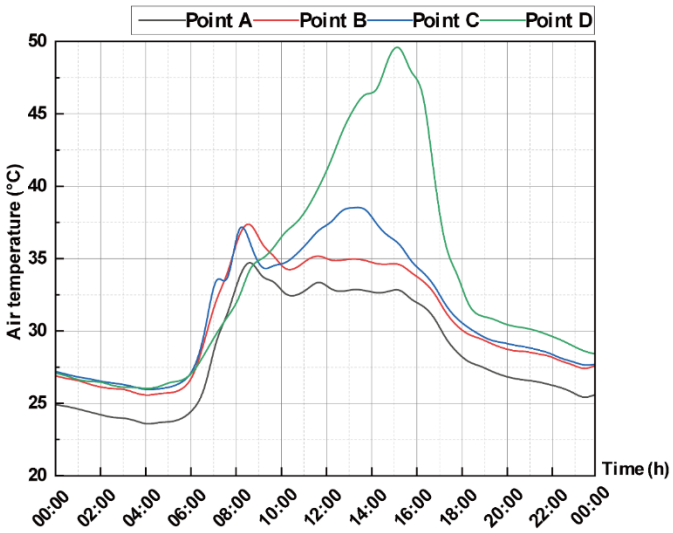

Figure 5 Air temperature measurement diagram for July 28, 2023 (source: by authors).

Figure 6 presents the full 24-hour relative-humidity (RH) profiles recorded by the four monitoring sensors on 28 July 2023. The diurnal cycle of humidity shows a clear sequence of phases, with both synchronized and divergent behaviors across the sites, reflecting differences in vegetation cover and surface characteristics.

From 00:00 to 01:00, all four curves remain stable at approximately 88 %, indicating uniform nocturnal conditions. A uniform decline follows between 01:00 and 03:00, with RH falling to 80 % at all sensors. At 03:30, a recovery phase begins, with RH values climbing steadily until 05:30. By this point, sensor A, situated in the most densely vegetated area (herbaceous plants, shrubs, and trees), reaches full saturation at 100 %, while the other sensors converge near 95 %. Between 05:30 and 07:30, this elevated plateau persists across all locations, maintaining an average of 94 %.

At 08:00, RH resumes a gradual climb. Sensors B, C, and D reach near-saturation (98 %) by 11:00, while sensor A peaks later, at 12:00, with a maximum of 99 %. The timing difference highlights a slight delay at the most densely greened site compared with the other three. After 12:00, a broad drying phase dominates the afternoon hours. Between 12:00 and 15:30, RH drops sharply, with amplitudes varying significantly by site: A declines to 60 %, B to 21 %, C to 35 %, and D to 21 %. This divergence illustrates the contrast between vegetated and non-vegetated surfaces, with site A maintaining the highest moisture levels and site D the lowest.

Between 15:30 and 19:00, a secondary moistening trend is observed. RH increases to 70 % at A, 55 % at B, 60 % at C, and 50 % at D, suggesting partial recovery of humidity in the evening. However, a subsequent decline occurs from 19:00 to 22:00. During this interval, RH falls again, bottoming at 65 % in A, 45 % in B, 50 % in C, and 40 % in D. After 22:00, radiative cooling initiates a final upward phase, raising RH values by the end of the day to 75 % in A, 60 % in B, 65 % in C, and 55 % in D.

Across the 24 hours, sensor D, located in the non-greened area, exhibits the largest amplitude of change, reflecting its stronger susceptibility to heating and drying during the day and reduced buffering at night. By contrast, sensor A demonstrates the most stable and consistently elevated RH curve, associated with its denser vegetation composition. Sensors B and C, representing intermediate greening levels, follow broadly parallel trajectories, though sensor C remains consistently 5–10 % higher than B during peak afternoon drying. This stratification across the four monitoring sites highlights the critical role of vegetation density in modulating near-surface humidity patterns under identical meteorological conditions.

Statistical comparisons support the observed humidity trends. Sensor A, with the densest vegetation, maintained the highest average RH over 24 hours at 80.1%, while Sensor D, located in a non-greened area, recorded the lowest at 60.7%, yielding a 19.4 percentage point difference. The diurnal RH range was widest at Sensor D (from 21% to 86%), compared to a much narrower band at Sensor A (58% to 100%), indicating that dense vegetation helps moderate humidity fluctuations.

The standard deviation of RH at Sensor A was ±15.7%, much lower than Sensor D's ±22.9%, revealing that vegetated zones offer more stable microclimatic conditions. Daytime RH (08:00–18:00) dropped sharply at D to an average of 43.7%, while A remained at 68.3%, demonstrating vegetation's capacity to retain atmospheric moisture during peak thermal stress periods.

These patterns are largely explained by evapotranspiration and canopy shading. Dense vegetation—especially herbaceous ground cover and shrubs in Sensor A—not only reduces direct solar radiation at the surface but also promotes continuous moisture release into the air through transpiration. This process enhances humidity and stabilizes the vapor balance of near-surface air. In contrast, the exposed surface at Sensor D heats and dries rapidly, lacking any moisture buffering capacity. This analysis highlights the microclimatic mechanisms through which vegetation density and stratification shape humidity profiles across time.

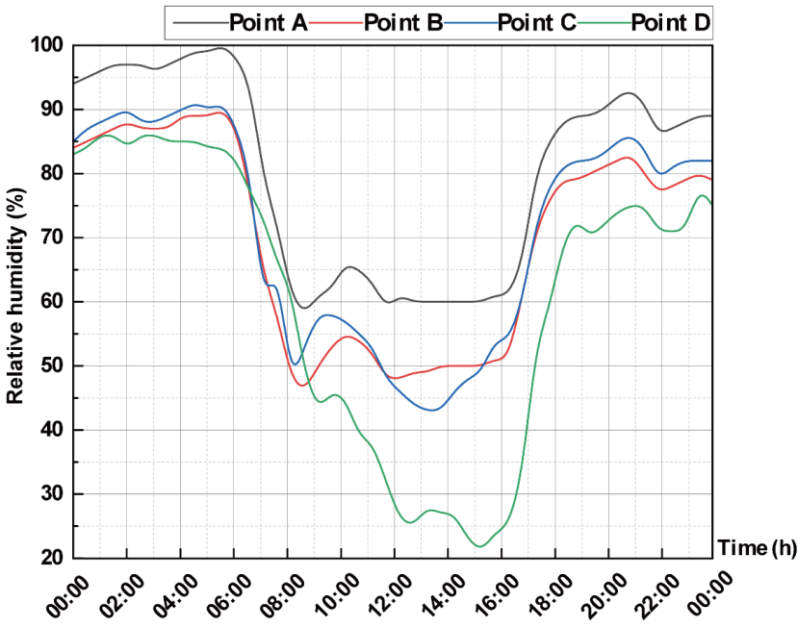

Figure 6: Relative humidity measurement diagram for July 28, 2023 (source: by authors).

4. Discussion

The comparative analysis of the four monitoring points (A: herbaceous plants, shrubs, and trees; B: shrubs and trees; C: trees only; D: no greening) provides important insights into how different greening structures influence the thermal and moisture environment in a traditional residential garden. The results show that vegetation complexity and surface cover strongly modulate both diurnal variability and the response to transient meteorological events.

1. Overall thermal and humidity dynamics: Across both cold and warm seasons, all four sensors exhibited clear diurnal cycles in air temperature and relative humidity. However, the amplitude, timing, and stability of these cycles varied significantly with vegetation composition. Point A, with the most diverse greening (herbaceous layer, shrubs, and trees), consistently showed the lowest air temperature and the highest relative humidity. This indicates that multiple vegetation strata provide synergistic cooling through shading and evapotranspiration, while also maintaining higher moisture levels. Point D, without greening, recorded the highest temperatures and lowest humidity, illustrating the destabilizing effect of bare or impervious surfaces. Points B and C fell between these extremes, with B generally cooler and moister than C, likely due to the additional shrub layer that contributes mid-level shading and transpiration.

2. Seasonal contrasts: Seasonal differences further highlight the role of greening. In winter, all sensors showed moderate thermal ranges, but vegetation-modulated responses were still evident. During snowfall, sensors with vegetation (A, B, and C) showed delayed and attenuated cooling compared to D, suggesting that canopy cover slowed the direct penetration of cold air and precipitation. Relative humidity increases were also strongest at A and B, where denser vegetation retained moisture longer. In summer, the influence of greening became much more pronounced. Sensor D, located on asphalt without greening, reached extreme temperatures above 50 °C, far exceeding vegetation points. In contrast, A peaked at only 33 °C, with much higher humidity. The nearly 17 °C difference between A and D demonstrates the substantial microclimatic contrast vegetation can create, even within a single garden. The gradient across A, B, C, and D reflects a direct link between vegetation structural complexity and thermal mitigation capacity.

3. Inter-point variability and vegetation structure: The stratification of greening appears to be a decisive factor. At point A, the presence of herbaceous plants in addition to shrubs and trees likely enhanced soil shading and reduced sensible heat flux from the ground, while transpiration from multiple vegetation layers maintained humidity stability. This produced the most buffered microclimate. At point B, the absence of herbaceous plants resulted in slightly higher temperatures and lower humidity than A, but the shrub and tree combination still provided significant moderation. Point C, with trees only, showed greater variability. Tree canopies reduced direct radiation but lacked the lower-layer shading and transpiration provided by shrubs and herbaceous plants, allowing greater heat accumulation near the surface. Point D, devoid of greening, was most exposed to solar radiation and precipitation, and thus exhibited the

largest amplitudes and volatility. This gradient underscores that vegetation effects are not binary (green vs. non-green) but scale with structural diversity and canopy layering.

4. Responses to meteorological events: Short-term weather events reinforced the vegetation effect. During winter snowfall, point D responded almost immediately with a temperature drop, while A, B, and C showed delayed responses, implying a buffering effect from canopy cover. Similarly, relative humidity increases occurred earlier and more sharply at A and B, likely due to the moisture retention and transpiration capacity of dense vegetation. In summer, transient cloud covers affect C more strongly, possibly because tree-only shading is more vulnerable to abrupt radiation changes than multi-layer systems. Precipitation events also induced synchronized cooling across all sensors, but the recovery rates differed: D rebounded fastest due to rapid surface heating, while A maintained cooler, moister conditions for longer. These differences confirm that vegetation layers not only reduce mean extremes but also modulate short-term microclimatic resilience.

5. Implications for outdoor thermal environment and comfort: The results indicate that multi-layered vegetation substantially improves outdoor thermal environments by lowering daytime heat and stabilizing humidity. In summer, this effect directly mitigates heat stress, with point A showing far more comfortable conditions than D. In winter, however, higher humidity in vegetated zones may reduce outdoor comfort, as cool and moist microclimates amplify perceived coldness. Thus, vegetation provides asymmetric benefits depending on season: strong thermal relief in summer, but potentially unfavorable conditions in winter. From a garden design perspective, this suggests that combining vegetation with careful spatial planning—such as locating seating near, but not directly under, dense canopy in winter—can optimize seasonal comfort.

6. Quantification of vegetation effects: Although the current study qualitatively identifies the microclimatic benefits of vegetation layering, future analysis should further quantify the effect magnitude by comparing average daytime and nighttime temperatures, relative humidity ranges, or diurnal fluctuation indices across greening types. Such data would enable clearer evaluation of thermal moderation performance. For instance, prior studies have suggested that the cooling effect of tree-shrub-herb layering can exceed that of single-layer tree planting, particularly under summer high-heat conditions. Establishing such metrics in small-scale residential gardens would greatly support landscape optimization strategies.

7. Integration with thermal comfort thresholds: To enhance the practical applicability of the findings, microclimatic data should be linked with human thermal comfort indicators, such as Physiological Equivalent Temperature (PET) or Universal Thermal Climate Index (UTCI), which are widely used to assess perceived comfort under different environmental conditions. This linkage can help determine when vegetation-induced cooling becomes thermally beneficial or when excessive humidity may reduce comfort, particularly in winter.

8. Policy and design implications: The empirical evidence from this study reinforces the potential of garden greening as a fine-scale climate adaptation strategy. Design guidelines for residential landscapes should emphasize the importance of structural vegetation diversity, recommending combinations of vertical layers (e.g., ground cover, shrubs, and trees) to maximize thermal regulation. Additionally, planning policies may consider incentivizing green retrofitting of existing private gardens, especially in high-density districts, where such microclimate interventions can have cumulative effects.

5. Conclusion

This study systematically examined the influence of different garden greening configurations on the outdoor thermal and moisture environment of a traditional Japanese residential garden. Four monitoring points with varying vegetation compositions—A (herbaceous plants, shrubs, and trees), B (shrubs and trees), C (trees only), and D (no greening)—were compared through continuous 24-hour field measurements in both winter and summer.

The results consistently demonstrated that vegetation modifies microclimatic conditions in measurable ways. Point A, with the most complex vegetation layering, exhibited the lowest air temperatures and highest relative humidity across both seasons. The buffering effect was evident in summer, where Point A's maximum temperature remained almost 17 °C lower than Point D, and relative humidity fluctuations were moderated. Point D, lacking any greening,

consistently showed the highest temperatures, lowest humidity, and greatest diurnal variability, reflecting direct exposure to solar radiation and precipitation. Points B and C displayed intermediate conditions, with B generally closer to A due to the presence of shrubs that enhanced shading and transpiration, while C, with trees only, exhibited larger fluctuations.

Seasonal contrasts highlighted the dual role of vegetation. In winter, vegetation moderated the immediate cooling effects of snowfall and retained higher humidity, producing more stable but cooler and moist conditions. In summer, vegetation markedly reduced heat stress, stabilized humidity, and limited extreme fluctuations, whereas Point D experienced extreme thermal stress on asphalt surfaces. Short-term meteorological events such as snowfall, rainfall, and cloud cover further reinforced the buffering capacity of vegetation, particularly at Points A and B.

Overall, the findings indicate that vegetation complexity and canopy layering strongly influence microclimatic conditions at the garden scale. Multi-layer vegetation not only reduces extreme temperature and humidity fluctuations but also delays and moderates responses to transient weather events. Conversely, the absence of greening produces high thermal and moisture volatility. These results provide quantitative evidence that vegetation structure plays a decisive role in shaping outdoor thermal environments within residential gardens.

These observations reveal that the cooling and humidifying effects of vegetation are notably more effective during summer, when thermal stress is most pronounced. Denser and more layered vegetation, such as the combination found at Point A, not only moderates temperature peaks but also helps maintain more stable moisture levels throughout the day. In winter, while the moderating effect is still present, the increased humidity and lower temperatures under vegetation can contribute to a cooler microclimate that may feel uncomfortable, especially in shaded or poorly ventilated areas.

From the perspective of human thermal comfort, these findings suggest that vegetation influences not only the physical environment but also the perceived thermal experience. Though formal indices such as the universal thermal climate index (UTCI) or PMV were not applied in this study, the observed patterns align with general comfort principles, namely, that excessive heat and dryness in summer and excessive dampness in winter can both reduce outdoor comfort. The study thus implies that optimal outdoor environments depend not only on the presence of vegetation but also on thoughtful planting design, spatial layout, and seasonal considerations.

In practical terms, this means that residential garden design should adapt vegetation structure to seasonal needs—for example, placing seating areas where summer shading is maximized, while allowing winter sunlight penetration. On a broader scale, the results support policies promoting multi-layered greening in urban settings, not merely for aesthetic or ecological reasons, but as a tool for enhancing environmental quality and thermal well-being in residential outdoor spaces.

6. Limitations and future work

This study has provided valuable insights into the microclimatic impacts of different garden greening configurations in a traditional Japanese residential context. However, several limitations should be acknowledged when interpreting the results.

First, the measurements were conducted at only four monitoring points with specific greening compositions: A (herbaceous plants, shrubs, and trees), B (shrubs and trees), C (trees only), and D (no greening). While these configurations represent common patterns in residential gardens, they do not encompass the full diversity of possible planting arrangements, such as groundcovers, vines, or different tree species with varying canopy densities. Consequently, the findings cannot be generalized to all forms of garden greening.

Second, the monitoring was performed during selected 24-hour periods in winter and summer. Although these timeframes captured seasonal contrasts, they did not cover longer-term variability such as transitional seasons (spring and autumn) or interannual differences. The influence of extreme weather events beyond those recorded—such as prolonged heatwaves, typhoons, or heavy snowfalls—was not examined, limiting the scope of inference regarding vegetation resilience under more severe climatic conditions.

Third, the study focused on air temperature and relative humidity as key indicators of the outdoor thermal environment. While these metrics are fundamental, other important microclimatic parameters, such as wind speed, surface temperature, and solar radiation, were not simultaneously recorded. These additional variables could provide a more complete understanding of the mechanisms through which vegetation modifies outdoor comfort.

Fourth, the research was restricted to a single traditional Japanese residential garden. Localized factors such as garden orientation, surrounding building geometry, and material properties may have influenced the results, making them less directly transferable to other residential settings, particularly those in different climatic zones or with different architectural forms.

In light of these findings, practical implications for residential landscape design and urban planning should be emphasized. The evidence indicates that multi-layered vegetation—combining herbaceous groundcovers, shrubs, and trees—offers superior thermal buffering and humidity stability, particularly during periods of climatic stress such as summer heat. Therefore, garden designs that integrate vegetation of varying heights and densities should be prioritized in residential projects seeking to enhance outdoor comfort. Urban greening policies could also incorporate these insights by encouraging structurally diverse plantings in both private and public spaces, aligning ecological benefits with thermal comfort outcomes.

Future research should therefore expand the spatial and temporal scope of field measurements. Including multiple garden sites with diverse planting designs and material surfaces would allow broader comparisons. Long-term monitoring across multiple seasons and years could also provide stronger evidence for the durability of vegetation effects. Incorporating additional microclimatic parameters such as radiation balance, wind dynamics, and soil moisture would further clarify the processes underlying thermal regulation. Finally, extending the analysis to cover subjective human thermal comfort alongside physical measurements could provide more comprehensive guidance for residential garden planning. And regarding future work, prioritizing research on transitional seasons (spring and autumn) could offer critical insights into vegetation performance under milder, yet rapidly changing, climate conditions. Additionally, groundcovers and vine-based greening systems remain underexplored but may offer efficient cooling with lower spatial requirements—making them highly relevant in space-constrained urban settings. Investigating these types using a combination of extended field measurements and simulation-based modeling tools, such as ENVI-met or CFD platforms, could significantly improve predictive capability. Future research should also seek to link microclimatic data with subjective thermal comfort surveys to bridge the gap between environmental measurements and human experience, enabling more user-centered design strategies.

Ackowledgment

The abstract of this paper was presented at the Urban Planning & Architectural Design for Sustainable Development (UPADSD) Conference – 10th Edition, which was held on the 21st- 23rd of October, 2025.

The authors gratefully acknowledge the support of the National Natural Science Foundation of China (Grant No. 52178083), the Taishan Scholars Young Experts Funding Program of Shandong Province (Grant No. tsqn202306236), Tianjin Science and Technology Plan Project (Grant No. 22JCZDJC00750), and the JST SPRING (Japan Grant No. JPMJSP2149).

Funding declaration

This research did not receive any specific grant from funding agencies in the public, commercial, or not-for-profit sectors/individuals.

Ethics approval

Not applicable.

Conflict of interest

The authors declare that there is no competing interest.

References

Bowler, D. E., Buyung-Ali, L., Knight, T. M., & Pullin, A. S. (2010). Urban greening to cool towns and cities: A systematic review of the empirical evidence. Landscape and urban planning, 97(3), 147-155.

Cannistraro, M., & Trancossi, M. (2019). Enhancement of indoor comfort in the presence of large glazed radiant surfaces by a local heat pump system based on Peltier cells. Thermal science and engineering progress, 14, 100388.

Hamada, S., & Ohta, T. (2010). Seasonal variations in the cooling effect of urban green areas on surrounding urban areas. Urban forestry & urban greening, 9(1), 15-24.

Heikkilä, M., & Hautamäki, R. (2024). Restorative environmental experiences: uncovering the invisible and visible attributes in Finnish forests and Japanese gardens-a literature review. Journal of Environmental Planning and Management, 1-22.

Klemm, W., Heusinkveld, B. G., Lenzholzer, S., & van Hove, B. (2015). Street greenery and its physical and psychological impact on thermal comfort. Landscape and urban planning, 138, 87-98.

Lin, H., & Li, X. (2025). The Role of Urban Green Spaces in Mitigating the Urban Heat Island Effect: A Systematic Review from the Perspective of Types and Mechanisms. Sustainability, 17(13), 6132.

Morakinyo, T. E., & Lam, Y. F. (2016). Simulation study on the impact of tree-configuration, planting pattern, and wind condition on street-canyon's micro-climate and thermal comfort. Building and environment, 103, 262-275.

Ng, E., Chen, L., Wang, Y., & Yuan, C. (2012). A study on the cooling effects of greening in a high-density city: An experience from Hong Kong. Building and environment, 47, 256-271.

Shashua-Bar, L., Pearlmutter, D., & Erell, E. (2011). The influence of trees and grass on outdoor thermal comfort in a hot-arid environment. International journal of climatology, 31(10), 1498.

Shen, L., Li, Y., Lan, S., & Yao, M. (2022). Social benefits evaluation of rural micro-landscapes in Southeastern Coastal Towns of China—The case of Jinjiang, Fujian. Sustainability, 14(13), 8036.

Spronken-Smith, R. A., & Oke, T. R. (1999). Scale modelling of nocturnal cooling in urban parks. Boundary-Layer Meteorology, 93(2), 287-312.

Zhang, G., Wu, Q., & He, B. J. (2021). Variation of rooftop thermal environment with roof typology: a field experiment in Kitakyushu, Japan. Environmental Science and Pollution Research, 28(22), 28415-28427.